An Experimental Study of the n-Si/Acetonitrile Interface: Fermi Level Pinning and Surface States Investigation

J.-N. Chazalviel* and T. B. Truong†

Contribution from the Laboratoire de Physique de la Matière Condensée,‡ Ecole Polytechnique, 91128 Palaiseau, France, and ERA 718, Laboratoire de Chimie Physique, Bât. 350, Université Paris-Sud, 91405 Orsay, France. *Received May 26, 1981*

Abstract: We present an experimental investigation of the n-Si/acetonitrile interface, in the presence of various redox systems and using several experimental techniques: current/voltage and capacitance/voltage characteristics, complex impedance, and photocurrent. In the absence of any redox system the conduction band potential is $V_c^0 = -0.75$ V referred to the Ag|0.01 M Ag^+ reference. In the presence of the redox systems the results indicate an evolution of the interfaces with immersing time, from an initial situation where the Schottky barrier height ϕ_B is nearly consistent with the classical expectation $\phi_B = e(V_{redox} - V_c^0)$, to a final situation where ϕ_B has an almost constant value $\approx$0.7 eV for all the redox systems. This is interpreted as a progressive transition from the classical "no pinning" regime, to the regime where the Fermi level is completely pinned in the bandgap by surface states. Direct investigation of the surface states by the subbandgap photocurrent technique confirms that the surface density of states increases with immersing time, in parallel with the evolution of ϕ_B. Complementary observations seem to indicate that the observed surface states are mainly due to slow surface oxidation of silicon.

The motivation for the present study is the search for Fermi-level pinning at the semiconductor/electrolyte interface. This effect has been known for a long time in solid-state metal–semiconductor junctions.[1] In these devices the Schottky barrier height ϕ_B, instead of following the expected variation $d\phi_B/d\phi \approx 1$ with the metal workfunction ϕ, is often found to be rather independent of the metal used.[2,3] This is commonly ascribed to the presence of surface states in the forbidden gap. If the density of these surface states is sufficiently large,[4] they can "pin" the Fermi level to a given position in the bandgap, independently of the adjacent metal. No clear-cut evidence for Fermi-level pinning at the semiconductor/electrolyte interface has been available for a long time. Recently, however, such observations have been reported independently by various groups on n- and p-GaAs,[5,6] p-Si,[7,8] and n-Si,[9] providing at the same time a simple interpretation for earlier experimental results.[10–12] Related surface-state effects have also been reported for transition metal dichalcogenides.[13–16] In a previous communication,[9] we reported our preliminary results showing a progressive transition from the unpinning regime to the full pinning regime at the n-Si/acetonitrile interface. In the present paper a detailed report of this work is given. A significant improvement in the present work is the use of various experimental techniques, including that of the subbandgap photocurrent, previously developed,[17] which allows direct observation of the surface states. In the Experimental Section we describe the experimental arrangement and techniques. The results are presented in the Results Section and discussed in the Discussion and Conclusion Section.

Experimental Section

The standard electrolyte that we used was acetonitrile (ACN) + 0.1 M tetrabutylammonium perchlorate (TBAP). Acetonitrile, a Merck Uvasol grade product, was left standing for 1 day on molecular sieves, then degassed through freeze–pump–thaw cycles, and finally vacuum distilled and stored under vacuum on activated molecular sieves. TBAP was dried under vacuum by heating at $\approx$50 °C for several hours. The solution was prepared shortly before use by vacuum distillation of $\approx$50 cm^3 of ACN on the TBAP in the preparation compartment. We used the following redox systems: ferrocene/ferricinium ($Fe(Cp)_2/Fe(Cp)_2^+$), cobaltocene/cobalticinium ($Co(Cp)_2/Co(Cp)_2^+$), chromocene/chromicinium ($Cr(Cp)_2/Cr(Cp)_2^+$), nickelocene/nickelicinium ($Ni(Cp)_2/Ni(Cp)_2^+$), benzoquinone/monoanion (BQ/BQ^-), anthraquinone/monoanion (AQ/AQ^-), and nitrobenzene/monoanion (NB/NB^-). (Standard potentials in volts vs. SCE are +0.31, −0.94, −0.67, −0.09, −0.51, −0.94, and −1.15, respectively, from the literature.[18,19]) The redox system was introduced in the form of the neutral species, preferably by vacuum distillation. In most cases the solution was preelectrolyzed to produce a comparable amount of the alternate species of the redox couple. For that reason the preparation compartment was designed as a balloon separated into two parts by a fine frit diaphragm (Figure 1). After preelectrolysis the prepared solution was transferred to a storage compartment, separated from the experimental cell by a stopper. In this way the solution was never in contact with air. The starting vacuum pressure was in the 10^{-2} torr range. The water content in the solutions, measured on several test solutions of ACN + 0.1 M TBAP by the Karl-Fisher method, was $\approx$15 μL of H_2O/L of solution.

The silicon sample was prepared as previously described.[20] It is to be noticed that the final HF rinse allows the sample to be handled in air for minutes without any appreciable oxidation, as can be checked for example by X-ray photoelectron spectroscopy or Auger electron spectroscopy.[20,21] The interface at the beginning of the electrochemical experiments is therefore essentially oxygen free.

* Ecole Polytechnique.
† Université Paris-Sud.
‡ Groupe de Recherche du Centre National de la Recherche Scientifique.

(1) J. Bardeen, *Phys. Rev.*, **71**, 717 (1947).
(2) C. A. Mead, *Solid-State Electron.*, **9**, 1023 (1966).
(3) E. H. Rhoderick, "Metal-Semiconductor Contacts", Clarendon, Oxford, 1978, pp 18–76.
(4) S. M. Sze, "Physics of Semiconductor Devices", Wiley, New York, 1969, pp 368–78.
(5) A. J. Bard, A. B. Bocarsly, F. R. F. Fan, E. G. Walton, and M. S. Wrighton, *J. Am. Chem. Soc.*, **102**, 3671 (1980).
(6) F. R. F. Fan and A. J. Bard, *J. Am. Chem. Soc.*, **102**, 3677 (1980).
(7) A. B. Bocarsly, D. C. Bookbinder, R. N. Dominey, N. S. Lewis, and M. S. Wrighton, *J. Am. Chem. Soc.*, **102**, 3683 (1980).
(8) J. A. Turner, J. Manassen, and A. J. Nozik, *Appl. Phys. Lett.* **37**, 488 (1980).
(9) J.-N. Chazalviel and T. B. Truong, *J. Electroanal. Chem.*, **114**, 299 (1980).
(10) D. Laser and A. J. Bard, *J. Chem. Phys.*, **80**, 459 (1976).
(11) A. B. Bocarsly, E. G. Walton, M. G. Bradley, and M. S. Wrighton, *J. Electroanal. Chem.*, **100**, 283 (1979).
(12) P. A. Kohl and A. J. Bard, *J. Electrochem. Soc.*, **126**, 59 (1979).
(13) H. Tributsch, H. Gerisher, C. Clemen, and E. Bucher, *Ber. Bunsenges. Phys. Chem.*, **83**, 655 (1979).
(14) W. Kautek, H. Gerisher, and H. Tributsch, *Ber. Bunsenges. Phys. Chem.*, **83**, 1000 (1979).
(15) L. F. Schneemeyer and M. S. Wrighton, *J. Am. Chem. Soc.*, **101**, 6496 (1979).
(16) A. J. Bard, F.-R. F. Fan, A. S. Gioda, G. Nagasubramanian, and H. S. White, *Faraday Discuss. Chem. Soc.*, No. **70**, 70/1 (1980), and references therein.
(17) J.-N. Chazalviel, *J. Electrochem. Soc.*, **127**, 1822 (1980).
(18) J. D. L. Holloway and W. E. Geiger, Jr., *J. Am. Chem. Soc.*, **101**, 203 (1979).
(19) C. K. Mann and K. K. Barnes, "Electrochemical Reactions in Nonaqueous Systems", Marcel Dekker, New York, 1970.
(20) J.-N. Chazalviel, *Surf. Sci.*, **88**, 204 (1979).
(21) J.-N. Chazalviel, to be published.

0002-7863/81/1503-7447$01.25/0

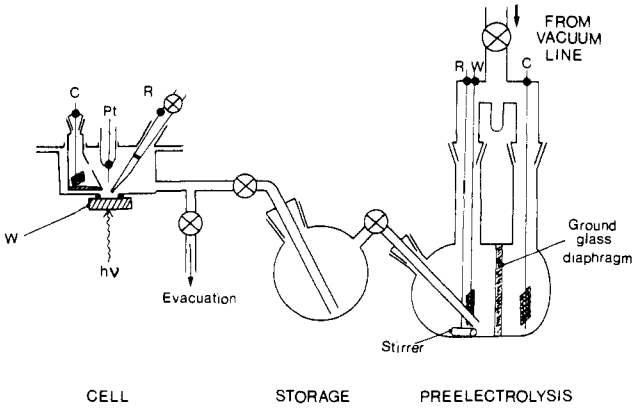

Figure 1. Scheme of the experimental arrangement.

Two designs were used for the electrochemical cell. In the first design the n-Si sample was enclosed in wax (except for the exposed surface) and mounted on a rotating electrode holder (the motor was of asynchronous type and the rotor was in vacuum so that no rotating hermetic feedthroughs were needed). In the second design the sample was simply pressed against an opening in the cell wall using an O-ring seal. The reference electrode was Ag|0.01 M $AgNO_3$|0.1 M TBAP in ACN and communicated with the main solution through a cracked quartz bead junction.[22] The reference electrode compartment was pumped at the same time as the main cell in order to avoid excessive flow rate through the junction. Electrode potentials quoted below are referred to this reference electrode, which is +0.3 V vs. aqueous SCE.[10,23]

The electrochemical measurements were performed with a classical three-electrode arrangement and a potentiostat. The interface was investigated by using several techniques: current/voltage characteristics $I(V)$, and capacitance/voltage characteristics $C(V)$ (hence the determination of the flat-band potential V_{fb} from the Schottky-Mott plot $1/C^2(V)$). The complex impedance $Z(V,\omega)$ at variable frequency $\omega/2\pi$ was measured in a few cases. The photocurrent ΔI_{ph} was also investigated, using chopped light excitation and lock-in detection, as a function of electrode potential V, monochromatic light wavelength λ, and chopping frequency $\omega/2\pi$. The subbandgap photoeffect ($hc/\lambda < E_g$) was studied with special interest, since it gives direct information on the surface density of states.[17] The analog measurements were sent to an analog digital converter, coupled with a Commodore PET 2001 microcomputer via an IEEE 488 bus. This allowed us to obtain routinely the Schottky-Mott plot from the $C(V)$ measurements, and the quantum yield/photon energy, $\eta(h\nu)$, curve from the photocurrent data.

Results

The results can be roughly summarized as follows. Two kinds of behaviors are observed: some interfaces are *nonrectifying*, i.e., voltammogram similar to that for a Pt electrode, and $V_{fb} \gtrsim V_{redox}$. Some other interfaces are *rectifying*, i.e., diode-like voltammogram and $V_{fb} \lesssim V_{redox}$. Furthermore the character of a given interface (i.e., rectifying or nonrectifying) is found to *change with time*, namely all the interfaces evolve toward the rectifying state. Before we come to a discussion of these results we first present them in detail, in the order of the different techniques that we used.

A. Current/Voltage Characteristics. Figure 2 shows the current/voltage characteristics for two representative interfaces, i.e., $Fe(Cp)_2/Fe(Cp)_2^+$ and AQ/AQ^-, as a function of immersing time. Scan rate is 10 V/min. The system $Fe(Cp)_2/Fe(Cp)_2^+$ gives the prototype of a rectifying interface (Figure 2b). It is rather stable with time. One may notice however an increase of the limiting anodic current, up to a broad maximum, followed by a slow decrease. AQ/AQ^- gives an example of a complete evolution from a nonrectifying to a rectifying behavior. At early times the voltammogram is similar to that obtained with a platinum electrode, i.e., it exhibits two symmetric peaks characteristic of a diffusion-limited current (curve 1 in Figure 2a). At larger immersing times the anodic peak decreases and broadens, then finally disappears and a small constant limiting current is obtained instead

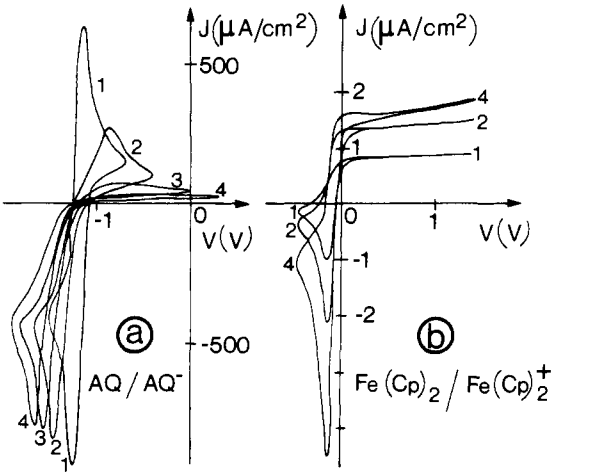

Figure 2. Voltammograms for two representative redox systems (a) AQ/AQ^- and (b) $Fe(Cp)_2/Fe(Cp)_2^+$ at different immersing times t: (1) t = 5 min, (2) t = 30 min, (3) t = 1 H, (4) t = 2 H. The increase of the cathodic peak in part b is due to the increase of the (initially zero) ferricinium concentration upon potential cycling.

(curve 4 in Figure 2a). The same behavior is obtained for $Co(Cp)_2/Co(Cp)_2^+$.[9] In the case of NB/NB^- and BQ/BQ^- the same behavior can be inferred but the evolution time scale is shorter in these cases, so that the initial fully symmetric voltammogram cannot be observed. On the other hand, in the case of $Cr(Cp)_2/Cr(Cp)_2^+$ the evolution is very slow and the final rectifying state is not reached even after hours of immersion. These results are shown in Figure 3a.

B. Capacitance/Voltage Characteristics. Flat-Band Potential. The capacitance measurements presented here are obtained by analog integration of the current peak obtained upon a ≈20-mV step variation of the electrode potential. The shape of the peak is monitored on the oscilloscope and only the data corresponding to a fast response capacitance (i.e., peak width $\lesssim$10 μs) are retained. This condition is fulfilled except in the vicinity of V_{fb}. These measurements are taken in the presence of various redox systems. The resulting flat-band potential V_{fb} is used to determine the conduction-band potential V_c:

$$V_c = V_{fb} - (kT/e) \ln (N_c/N_D)$$

and the Schottky barrier height $\phi_B = e(V_{redox} - V_C)$. (Here N_D is donor concentration and N_C is the equivalent density of states for the conduction band; $N_C = 2.8 \times 10^{19}$ cm^{-3} for silicon at 297 K.[24]) The obtained ϕ_B is plotted in Figure 3b. For $Fe(Cp)_2/Fe(Cp)_2^+$ the conduction-band potential is stable with time and is the same as in the absence of any redox system, $V_c^0 \approx -0.75 \pm 0.03$ V. In the other cases V_c is found to shift increasingly with increasing immersing time toward more negative values. In all cases the value of ϕ_B at long immersing time is found to approach a common limit $\phi_B \approx 0.7$ eV. This can be taken as evidence for Fermi-level pinning at the Si surface.[9] Since this pinning occurs progressively with immersing time, it is to be expected that the surface states responsible for pinning are initially absent and arise from the contact with the electrolyte.

C. Photocurrent. (i) The photocurrent induced by *bandgap light* irradiation is measured using chopped light and a lock-in detection. The light intensity is kept very weak as large intensities were found to alter the interface noticeably.[25] The photocurrent/potential curve rises in about 0.2 V from zero up to a plateau (see Figure 4). The value of the plateau corresponds, within a factor of 2, to complete collection of the photoholes generated within a diffusion length from the surface (absorption in the space charge layer is negligible). The potential for the rising edge, measured at half-height, $V_{1/2}^{ph}$, is found in all cases to be at +0.35

(22) D. T. Sawyer and J. L. Roberts, Jr., "Experimental Electrochemistry for Chemists", Wiley, New York, 1974, p 27.
(23) A. K. Covington and T. Dickinson, "Physical Chemistry of Organic Solvent Systems", Plenum, London, 1973, pp 196–7.
(24) R. A. Smith, "Semiconductors", Cambridge University Press, New York, 1968, p 359.
(25) T. B. Truong and J.-N. Chazalviel, to be published.

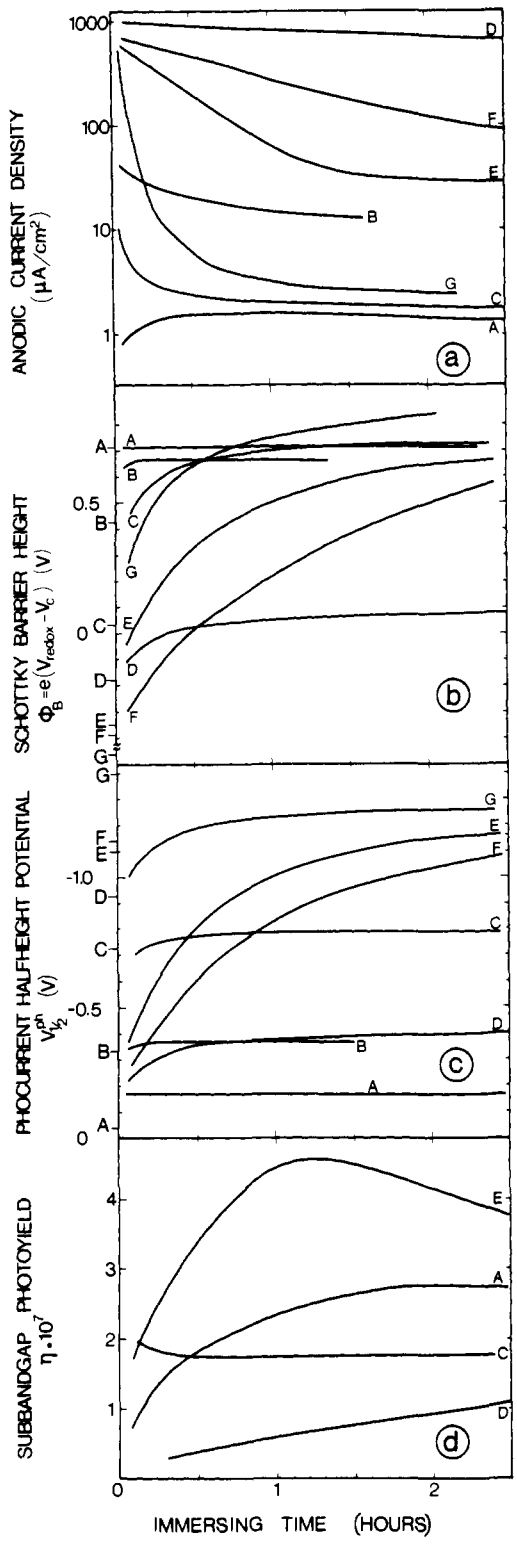

Figure 3. Typical results for the various redox systems, (A) $Fe(Cp)_2/Fe(Cp)_2^+$, (B) $Ni(Cp)_2/Ni(Cp)_2^+$, (C) BQ/BQ^-, (D) $Cr(Cp)_2/Cr(Cp)_2^+$, (E) AQ/AQ^-, (F) $Co(Cp)_2/Co(Cp)_2^+$, (G) NB/NB^-, as a function of immersing time. Concentrations of the redox species are $\sim 10^{-2}$ M. (a) Maximum anodic current: data above ~ 100 $\mu A/cm^2$ correspond to an anodic peak; data below that value correspond to a nearly constant limiting current. (b) Schottky barrier height deduced from the V_{fb} measurements. On the left-hand scale are shown the expected values for no pinning. (c) Half-height photocurrent potential measured as shown in Figure 4. The redox potentials are shown on the left-hand scale. (d) Subbandgap photocurrent quantum yield measured at $h\nu = 0.8$ eV. The absolute scale is valid within a factor of 2.

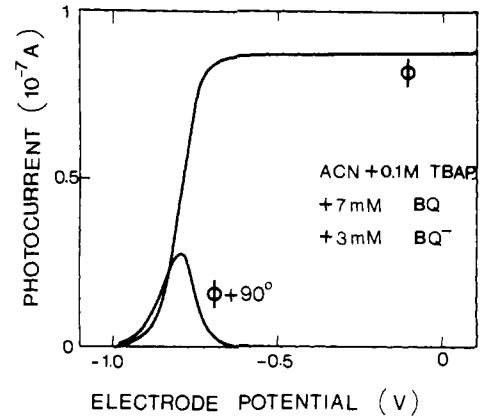

Figure 4. Typical photocurrent/potential curve. Light is chopped at 35 Hz. The curve is shown for two settings of the lock-in phase (see text), $h\nu \approx 1.0$ eV.

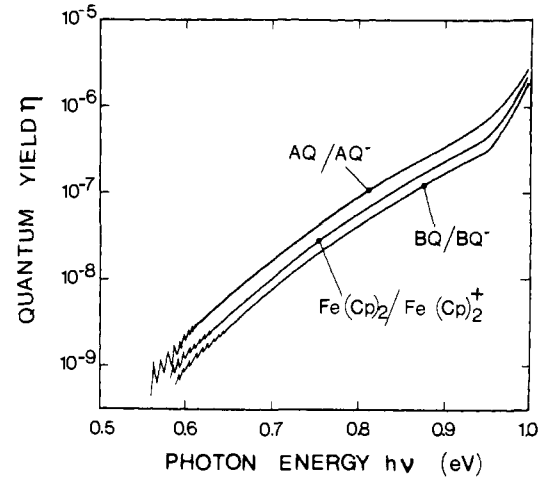

Figure 5. Quantum yield (number of photoelectrons per incident photon) for the subbandgap photoeffect. $V - V_{redox} = +1$ V. Notice the similarity of the curves for the different redox systems.

± 0.10 V positive of the flat-band potential. This is measured at 35 Hz light chopping frequency. We actually observe a dependence of the photoeffect upon the frequency of light chopping in this potential range. This frequency dependence, associated with the out-of-phase signal shown in Figure 4, also results in a small decrease of $V_{1/2}^{ph}$ with increasing chopping frequency. For a given redox system the range spanned by $V_{1/2}^{ph}$ from dc to 1 kHz is typically 0.1 to 0.2 V wide. Figure 3c shows the time variations of $V_{1/2}^{ph}$ measured at 35 Hz chopping frequency for different redox systems. The variations of $(-V_{1/2}^{ph})$ are seen to follow nicely those of ϕ_B (Figure 3b).

(ii) More interesting is the photocurrent induced by subbandgap light irradiation: As it was previously shown[17] subbandgap light may induce transitions between surface states and the semiconductor bands. The resulting photoeffect gives direct information on the surface states. The dependence of the subbandgap quantum yield upon photon energy that we observe in ACN electrolytes (Figure 5) is very similar to that previously observed in aqueous electrolytes.[17] This implies a similar energy distribution for the states in the gap and possibly a common origin in these two systems. The dependence of the subbandgap photocurrent upon electrode potential is also similar to that observed in aqueous electrolytes, i.e., it differs from that of the bandgap photocurrent only by a small increase in the region where the bandgap photocurrent is constant (this was previously ascribed to a barrier lowering effect).[17] The subbandgap photocurrent depends upon the frequency of light chopping just like the bandgap photocurrent.

A most interesting observation is that of the time dependence of the subbandgap photocurrent. This result is shown in Figure 3d, for a light energy $h\nu = 0.8$ eV. In most of the investigated

systems the photoyield is found to increase with increasing time, up to a plateau followed by a very slow decrease. The time scale of the increase correlates with the time scale for the change in V_{fb} or the change in the dark anodic current. This gives strong support to the above statement that *the surface states responsible for pinning are initially absent and arise from the contact of the surface with the electrolyte.*[26] The fact that the subbandgap photoyield extrapolates reasonably well to zero at $t = 0$ is a good check for initial surface preparation. The slow decrease of the subbandgap photoeffect at long immersing times can be understood as an effect of oxidation.

A special mention can be made here on the case of ferrocene. In this case not only the subbandgap photocurrent, but also the dark anodic current initially increases, a unique feature in Figure 3a. Such a behavior might be due to a decrease with time of the Schottky barrier height. The latter, however, is found to be remarkably constant (Figure 3b). A plausible explanation is that the dark anodic current also involves the surface states as transfer intermediates[27] and therefore increases in parallel with the surface states density. For other redox systems, the increase of ϕ_B with time is the leading effect, hence the decrease of the dark current with time.

D. Complex Impedance. The complex impedance of the interface $Z(V,\omega)$ was measured for some of the cited redox systems. For the system $Fe(Cp)_2/Fe(Cp)_2^+$ the impedance data are essentially similar to those one would obtain with a metal/semiconductor junction; i.e., a reasonable approximation for the equivalent circuit is the capacitance of the space charge layer in parallel with a resistance varying with electrode potential as $\exp(+eV/kT)$. For the system BQ/BQ^- and other systems where V_{fb} is strongly shifted from its initial value, the impedance data are less simple; namely there is a range in ω and V where the junction behaves as a capacitance $\sim 1\ \mu F/cm^2$, much larger than that of the space charge layer C_{sc} (for our samples $C_{sc} \sim 10$ nF/cm^2). This range in ω and V is further found to correspond to that where the bandgap photoeffect depends upon the frequency of light chopping (see above paragraph and Figure 4). We think all these observations can be accounted for if the electrochemical charge transfer is assumed to take place via the intermediate of the surface states. These data, together with a detailed quantitative model, will be discussed in a separate theoretical paper[27] and are therefore excluded from the following discussion.

Discussion and Conclusion

A. The experimental results are summarized in Figure 3. The emerging picture, already mentioned above, is rather clear: at short immersing times the surface density of states, measured by the subbandgap photoeffect, is small (Figure 3d), the flat-band potential V_{fb} and photocurrent half-height potential $V_{1/2}^{ph}$ are insensitive to the redox system (Figures 3b and 3c), the Schottky barrier height is $\phi_B^0 = e(V_{redox} - V_c^0)$, and the interface is rectifying or nonrectifying (Figure 3a) depending upon the position of the redox potential relative to the conduction-band potential $V_c^0 = -0.75$ V. As time increases, so does the surface density of states (Figure 3d) and the potentials V_{fb} and $V_{1/2}^{ph}$ simultaneously shift from their initial values (Figures 3b and 3c). At long immersing times V_{fb} and $V_{1/2}^{ph}$ differ from V_{redox} by only a constant term, and the Schottky barrier height is almost constant, $\phi_B \approx 0.7$ V, i.e., *complete Fermi-level pinning* is obtained. This is verified by the rectifying $I(V)$ characteristics obtained for nearly all of the redox systems (Figures 3a and 2). The scheme for the interface at equilibrium at various stages of this evolution is shown in Figure 6a for a redox system giving initially a nonrectifying behavior. Figure 6b gives a scheme for the corresponding situations under strong anodic polarization. It is intended for the discussion of the quantitative meaning of the V_{fb} measurements (see Appendix).

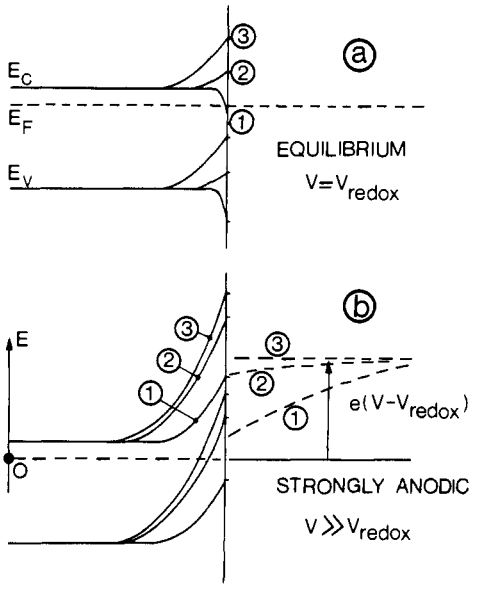

Figure 6. Scheme of the interface for a redox system with $V_{redox} < V_c^0$ at various stages of Fermi level pinning (left: semiconductor; right: electrolyte): (1) no surface states; (2) intermediate surface density of states; partial pinning; (3) large surface density of states; complete pinning. The heavy lines are for the semiconductor bands. The dashed lines are for the Fermi level. (a) Interface at equilibrium (constant E_F). (b) Interface under strong anodic bias. The variation of E_F inside the electrolyte is associated with the regime where the current is limited by diffusion of the redox species (see Appendix).

B. In order to elucidate the chemical nature of the surface states present at the n-Si/ACN interface, we have performed some complementary experiments, discussed hereafter. Further observations on purposely oxidized surfaces will be reported elsewhere.[25] (i) We have found that rotating the n-Si electrode increases the evolution rate of the surface. This indicates that the species in the solution responsible for the formation of the surface states is a *dilute* species rather than the solvent itself. (ii) In the case of a solution contaminated with air or water, the evolution rate is also found to increase. (iii) Omitting the HF rinse of the n-Si sample prior to the experiment is found to give a surface similar to that observed usually after hours, i.e., complete pinning and subbandgap photocurrent slowly decreasing.[25] Since such a surface is known to be covered by 5–10 Å of SiO_2, this suggests that one of the main causes for the observed surface states is slow oxidation of the surface by traces of water or oxygen present in the solution. An order of magnitude estimate indeed shows that if species present in the solution in a concentration $C \sim 1$ ppm and diffusion coefficient $D \sim 10^{-5}$ cm^2/s are adsorbed on the surface with unit sticking coefficient, the thickness of the built layer in a time τ as short as 10^2 s will be of the order of $C\sqrt{D\tau} \sim 3$ Å, that is typically a monolayer!

At this point one may wonder whether or not part of the observed surface states are induced by adsorbed species of the redox couples. The concentration of these species is typically one order of magnitude larger than that of water (1 mM = 18 ppm of H_2O/volume) and in view of the literature on derivatized silicon electrodes,[11,28,29] adsorption of the redox species may be expected. If so, the presence of such adsorbed species might induce electronic

(26) The present data might alternately be interpreted by invoking a filling (change of population) of preexisting surface states upon contact with the redox electrolyte. We think this alternate interpretation can be dismissed for the following reasons: (i) For a given redox system (e.g., NB/NB^- or AQ/AQ^-) the characteristic time for pinning seems to be rather insensitive to the concentrations of the redox species. (ii) Bandgap irradiation of oxidized surfaces causes hole trapping in the surface states, thereby decreasing the magnitude of the subbandgap photoeffect (see ref 17 and 25); turning the bandgap light on and off hence provides a technique for measuring directly the equilibration time of the surface states population. This time is found to be smaller than the lock-in response time (0.3 s) except for strongly oxidized surfaces. This value is clearly incompatible with the ~1 h time for Fermi level pinning.

(27) J.-N. Chazalviel, to be published.

(28) M. S. Wrighton, R. G. Austin, A. B. Bocarsly, J. M. Bolts, O. Haas, K. D. Legg, L. Nadjo, and M. C. Palazzotto, *J. Am. Chem. Soc.*, **100**, 1602 (1978).

(29) J. M. Bolts, A. B. Bocarsly, M. C. Palazzotto, E. G. Walton, N. S. Lewis, and M. S. Wrighton, *J. Am. Chem. Soc.*, **101**, 1378 (1979).

surface states in the semiconductor gap.[17,30] The different evolution rates from one redox system to another (see Figure 3) would then be ascribed to the different adsorption rates of the various species. If alternately the surface states are exclusively ascribed to oxidation, the observed evolution rates can however be accounted for by the changes in water or oxygen concentration, due to chemical reactivity of the redox species: when extremely oxidizable materials like cobaltocene[31] or chromocene[31] are present, they may act as very efficient O_2 and/or H_2O scavengers in the solution, the reaction products being eliminated as insoluble oxides or hydroxides, and the silicon oxidation is subsequently slowed down. The opposite effect is obtained with such species as BQ^-, NB^-, and to a lesser extent AQ^- because these also react with oxygen and water, but among the reaction products are OH^- ions,[19,25] which are known to speed up silicon oxidation.[17,20] Thus far we cannot therefore conclude whether or not adsorption of redox species contributes to surface states formation. In order to answer this question a better dehydratation of the solutions would be highly desirable. In any case the contribution of silicon oxidation has been ascertained.

In conclusion, we have investigated the n-Si/acetonitrile interface in the presence of different redox systems and using various techniques. We observe a change of the interface with immersing time from a "no-pinning" regime to a regime where the surface Fermi level is completely "pinned" by surface states: (i) evolution of the flat-band potential and photocurrent onset potential toward values depending upon the redox system, the final value of the Schottky barrier height being roughly a constant $\phi_B \approx 0.7$ eV, (ii) parallel evolution of the $I(V)$ characteristics toward a common rectifying behavior, and (iii) parallel increase of the subbandgap photoyield, indicating an increase with time of the surface density of states. Additional observations show that these surface states are at least partially induced by the beginning of oxidation of the silicon surface.

Acknowledgment. We are indebted to Dr. Combelasse and Drs. Lecayon and Le Moët for kindly performing the Karl–Fisher test experiments.

Appendix. On the Quantitative Meaning of the Flat-Band Measurements

The flat-band potentials discussed in this paper are determined from capacitance measurements performed in the presence of the redox systems, and in some instances, in a situation where the Faradaic current is limited by *ion diffusion* in the electrolyte. Such a situation may arise for the systems with $V_{redox} < V_c^0$, for example AQ/AQ^-. In this case the composition of the electrolyte is deeply changed in the vicinity of the interface. This may cast some doubt on the quantitative meaning of the flat-band potential and the deduced Schottky barrier height obtained in such conditions. We address this problem in the following. We distinguish three cases, according to the density of surface states, and corresponding to curves 1, 2, and 3 in Figure 6. (i) If no surface states are present (curves 1 in Figure 6) the matching condition at the interface is simply continuity of the *electrostatic potential*. Under anodic polarization the current will be limited by ion diffusion and the Fermi level will vary in the solution according to Nernst law

$$E_F = E_{redox} + kT \ln (C_{red}/C_{ox})$$

where C_{red} and C_{ox} are the concentrations of the reduced and oxidized species, respectively. The electrostatic potential will however stay constant through the solution and the position of the conduction band at the surface will simply follow the variations of eV, i.e., the flat-band potential will be the same as in the absence of any redox system.

(ii) At the other extreme if the surface density of states is very large (curves 3 in Figure 6) the matching condition is that the *Fermi level* at the surface must be at a fixed distance (here $\phi_B \approx 0.7$ eV) below the conduction band. This is the classical "Fermi-level pinning" effect. (Only a very small deviation from this condition is needed to provide a sizable surface charge, allowing the electrostatic potential to have a jump through the interface.) In this case however the anodic current will be limited by the diode and the Fermi level will be constant through the solution. The measured V_{fb} will then be, as expected, $V_{fb} = V_{redox} - (\phi_B/e) + (kT/e) \ln (N_C/N_D)$ and the resulting value of the Schottky barrier will be correct.

(iii) The most difficult case is that of an intermediate surface density of states, i.e., the case of *partial Fermi-level pinning*. In the latter case it may happen that the anodic current is still limited by ion diffusion and the Fermi level changes through the solution as in case i (curves 2 in Figure 6). But now the position of the conduction band at the surface is determined *partly by the electrostatic potential, and partly by the position of the Fermi level*. When simple electrostatics is used, this can be written in the following form, essentially equivalent to eq 24 and 22b of ref 4:

$$E_c = \{[e(V - V_{redox}) + \phi_B^0] + \alpha[E_F + \phi_B^\infty]\}/(1 + \alpha)$$

where ϕ_B^0 is the initial (no pinning) value of the Schottky barrier, ϕ_B^∞ is the value with complete pinning, and α is a dimensionless parameter proportional to the surface density of states.[4] The position of the surface Fermi level will in practice decrease down to a position where the diode reverse current equals the diffusion current, i.e., $E_F = E_C - \phi_B'$, where ϕ_B' is a function of the diffusion current. This gives

$$E_C = e(V - V_{redox}) + \phi_B^0 + \alpha(\phi_B^\infty - \phi_B')$$

Hence by using the true value of the barrier[4] $\phi_B = (\phi_B^0 + \alpha\phi_B^\infty)/(1 + \alpha)$ it gives

$$E_C = e(V - V_{redox}) + \phi_B + \alpha(\phi_B - \phi_B')$$

This means that the measured V_{fb} is shifted by a negative amount $\alpha(\phi_B - \phi_B')/e$ from its correct value. This correction vanishes in the two extreme limits ($\alpha = 0$ if no pinning, $\phi_B - \phi_B' = 0$ if the limiting current is smaller than the ion-diffusion current). The intermediate case measurements (Figures 3b and 3c) can only be given a qualitative meaning, unless a model is taken to estimate ϕ_B'.[32]

(30) S. R. Morrison, "The Chemical Physics of Surfaces", Plenum Press, New York, 1977, Chapters 5 and 7.

(31) G. E. Coates, M. L. H. Green, P. Powell, and K. Wade, "Principles of Organometallic Chemistry", Halsted, Wiley, New York, 1968.

(32) Rotating the electrode should in principle change the value of the ion diffusion current hence ϕ_B' and the observed V_{fb}. We were however unable to observe such changes unambiguously, especially because of the large evolution rate of the surface when the electrode is rotating.